Vol 2, No 2, pp. 67–77, 2010
International Journal of
Mathematical and Computational
Forestry & Natural-Resource Sciences

AVAILABLE ONLINE AT HTTP://MCFNS.COM

Submitted: Feb. 3, 2010
Accepted: Jun. 12, 2010
Published: Aug. 28, 2010
Last Correction: Aug. 11, 2010

A MONTE CARLO METHODOLOGY FOR SOLVING THE OPTIMAL TIMBER HARVEST PROBLEM WITH STOCHASTIC TIMBER AND CARBON PRICES

Stanislav Petrášek[1], John Perez-Garcia[2],
[1]*Ph.D. Student,* [2]*Professor, School of Forest Resources, University of Washington, Seattle, WA 98195 USA*

Abstract. This article presents a Monte Carlo methodology for solving the stochastic optimal timber harvest problem modeled as a recurrent American call option. A detailed description of the proposed methodology is given, and the Monte Carlo technique is contrasted with finite difference methods typically used to find solutions of the optimal harvest problem with stochastic prices. The use of the methodology is then demonstrated via an example. In the example, expected bare land values and optimal harvest policies are calculated for a Douglas-fir stand in western Washington State. It is assumed that the forest owner derives revenue from traditional timber sales and carbon sequestration, and that prices of timber and carbon follow a known stochastic process. Results of the calculations are discussed.

Keywords: Optimal Harvest, Carbon Sequestration, American Option, Monte Carlo

1 Introduction

The optimal harvest problem is of fundamental importance to forest economics and has been studied extensively for many years. A rich body of literature exists on determining the optimal harvest age and value of a forest stand under different conditions. Traditionally, the analysis has been performed under the assumption that prices of timber are known and do not change over time. However, since the 1970's, some researchers have been focusing their attention on the optimal harvest problem with stochastic timber prices.

One of the earliest articles to analyze the impact of stochastic timber prices on stand values and rotation lengths was presented by Norstrom 1975. This work was followed by other articles, for example those by Kaya and Buongiorno 1987 and Lohmander 1987. Arguments for an explicit treatment of stochastic timber prices and a review of existing literature were presented by Newman 1988, and many additional articles were published in the following decade. Among these were the articles by Morck et al. 1989, Haight 1993, and Plantinga 1998. A review of the existing literature on forest management in the presence of risk and uncertainty was given by Brazee and Newman 1999.

The articles by Morck et al. 1989 and Plantinga 1998 were two among several that analyzed the stochastic optimal harvest problem using real options methodology, an approach that applies ideas originally introduced in financial economics to the valuation and optimal management of real assets under uncertainty.[1] Two more recent examples characteristic of the use of the real options methodology in forest economics are the articles by Insley 2002 and Insley and Rollins 2005, who modeled the single and multi-rotation stochastic optimal harvest problems as American call options, a type of contract that gives its holder the right, but not the obligation, to harvest a forest stand at a given age. (For an introduction to options see, for example, the text by Hull 2003). Another recent example of a real options approach to risk management in forestry is provided by an article by Chladna 2007, who analyzed a stand management scenario where the forest owner receives revenue not only from timber but also from carbon emission permits.

Application of real option methodology to the stochastic optimal harvest problem typically yields a partial differential equation that must be solved numerically subject to a set of conditions in space and time. Traditionally, the numerical solution techniques used in option valuation have employed finite difference schemes. The article by Insley and Rollins 2005 is perhaps the best example of this approach. Chladna 2007 did not specify the details of the methodology actually used to obtain the results of her study, but the partial differential equa-

[1] A thorough introduction to real options can be found in the texts by Dixit and Pindyck 1994, and Trigeorgis 1996.

tions that she derived could also be solved with finite difference schemes.

Finite difference methods are not the only methodology that can be employed in the valuation of real options. As discussed, for example, by Glasserman 2004, a viable alternative is provided by algorithms based on Monte Carlo methods. From a theoretical perspective, the two approaches are equivalent in their ability to calculate option values. However, in the variety of problems considered in practical applications, some are more easily solved with a finite difference scheme, while a Monte Carlo algorithm is a preferable choice for others.

The goals of this article are twofold. First, a Monte Carlo algorithm capable of solving the multiple rotation optimal harvest problem with two sources of uncertainty is presented. The algorithm is an adaptation of the method introduced by Ibáñez and Zapatero 2004 for the valuation of financial American options, with modifications that extend the original method to infinite time horizons and multiple rotations. Second, the use of the extended algorithm is illustrated in a practical setting. The algorithm is used, in a scenario similar to that analyzed by Chladna 2007, to determine the value and optimal harvest schedule for a Douglas-fir site in western Washington State, under the assumption that the traditional income from timber sales is supplemented by income from carbon sequestration.

The article is organized as follows. The logic of the recursive Monte Carlo method employed throughout the article is first introduced in Section 2 for the simplest case of a single-rotation, optimal harvest problem with stochastic timber prices. Section 3 introduces the case with $N > 1$ rotations and the modifications that are required before the method can be used to calculate bare land values and optimal timings in a multi-rotation setting. This is followed in Section 4 by a presentation of the multi-rotation method in the context of a stochastic optimal harvest problem with two sources of uncertainty. Finally, in Section 5, the two-dimensional, multi-rotation version of the method is applied to an illustrative problem, and the solution is presented and discussed in Section 6.

2 Wicksellian Harvest Problem and Monte Carlo

As discussed, for example, by Plantinga 1998 and Insley 2002, the optimal timber harvest problem can be formulated as an American-style real option. The option formulation allows for the explicit treatment of stochastic timber prices, and it leads to harvest problem solutions in the form of expected bare land values and associated optimal harvest boundaries. These solutions are typically obtained with the use of various finite difference methods. However, algorithms based on Monte Carlo methodology provide a flexible alternative for calculating option values, of particular use in fields such as forest management, where the options of interest are characterized by multiple sources of uncertainty and complex payoffs and optimal harvest policies.

The Wicksellian (*i.e.*, single rotation) optimal harvest problem with stochastic timber prices can be thought of as an American call option on the value of timber. It is particularly amenable to solution by Monte Carlo simulation, because it can be posed as the expectation maximization problem

$$\pi(S_0, C) = \sup_{\tau^* \in \mathbb{R}^+} \mathbb{E}[d_0^{\tau^*} Q_{\tau^*} (S_{\tau^*} - C)^+ | S_0, C], \quad (1)$$

where $\pi(S_0, C)$ stands for the expected discounted value of a harvest that will take place at a future date for given values of harvest cost C and starting price S_0, the supremum is taken over the harvesting times that assume values in the set of positive reals $\mathbb{R}^+$, τ^* is the optimal harvest time, $\mathbb{E}[\cdot|\cdot]$ represents the conditional expectation operator, $d_0^{\tau^*}$ is the discount factor from time τ^* to present, Q_{τ^*} denotes the timber volume specified by the yield function Q_t at the optimal harvest time $\tau*$, and S_{τ^*} denotes the stochastic price of timber per unit volume. The term $(S_{\tau^*} - C)^+ = \max[S_{\tau^*} - C,\ 0]$ and indicates that the stand is never harvested in periods when harvest cost exceeds timber price. Equation 1 states that in order to maximize the profit from a single harvest, a forest owner must maximize the expected discounted harvest profit by selecting harvest time in response to price fluctuations.

The expected present value of harvest $\pi(S_0, C)$ in Equation 1 can be approximated by a Monte Carlo algorithm introduced by Ibáñez and Zapatero 2004. As is the case with all American-style options, the algorithm produces a solution that consists of both the option value $\pi(S_0, C)$ and the associated optimal harvest boundary B_t, which determines the minimum harvest price at which the stand should be harvested.

Several assumptions must be made before the Ibáñez and Zapatero 2004 algorithm can be applied to the single rotation optimal harvest problem with stochastic timber prices. The first of these assumptions concerns the treatment of time. Although time is assumed to be continuous in Problem 1, it is treated as discrete in the presentation that follows. The switch from continuous to discrete time is necessitated by the properties of the Ibáñez and Zapatero algorithm. It is also a realistic representation of the decisions made by forest owners, who may not be able to harvest a stand at all times due to, for example, high fire risk or extreme cold. The yield function Q_t is assumed to be a known and deterministic function of time. Similarly, the discount factor d_0^{τ} is

also assumed to be known with certainty for any value τ^*. The harvest cost C is known and constant over time. Finally, timber prices follow a diffusion process (see, for example, the text by Iacus **?**) whose dynamics can be described by the stochastic differential equation

$$dS_t = b(t, S_t)\, dt + \sigma(t, S_t)\, d\mathbb{W}_t\,, \tag{2}$$

where $b(t, S_t)$ represents the deterministic drift coefficient, $\sigma(t, S_t)$ represents the volatility coefficient, and $d\mathbb{W}_t$ is an increment of the Wiener process. Equation 2 can be discretized, or in some cases solved analytically, and used to generate price paths used by the valuation algorithm.

Because the Ibáñez and Zapatero algorithm relies on backward recursion, it is necessary to set an upper time limit T on the value of τ^* before the method can be applied to the infinite horizon Problem 1. The choice of T is determined as a tradeoff between minimization of the error caused by the truncation on the one hand, and computational cost on the other. For a given value of T, the time horizon is divided into an arbitrarily large number of time intervals, and it is assumed that the stand can only be harvested at the values of $t \in \{0, 1, 2, \ldots, T-1, T\}$ separating these intervals.

Ibáñez and Zapatero showed that once the optimal harvest boundary B_t is known at each $t \in \{0, 1, \ldots, T\}$, the option value $\pi(S_0, C)$ given in Equation 1 can be approximated by the Monte Carlo simulation

$$\begin{aligned}\pi(S_0, C) \approx \frac{1}{M}\sum_{i=1}^{L} d_0^{\tau^*} Q_{\tau^*}(S^i_{\tau^*} - C) \\ + \frac{1}{M}\sum_{j=1}^{K} d_0^T Q_T (S_T^j - C)^+\,,\end{aligned} \tag{3}$$

where τ^* denotes the first time in $\{0, 1, \ldots, T\}$ such that $S^i_{\tau*} \geq B_{\tau^*}$ – that is, the first time a simulated price path i exceeds the optimal harvest boundary. In Simulation 3, $M = K + L$ represents the total number of price paths simulated from Equation 2, L represents the number of price paths that induced harvesting at times $\tau^* < T$, K is the number of price paths where $\tau^* = T$, d_0^T represents the discount factor from T to 0, S_T^j is the value of j^{th} price path at time T, and all other terms are defined as above.

Figure 1 provides a simple illustration that highlights the key characteristics of Simulation 3. In Figure 1, starting price $S_0 = 400$, harvest cost $C = 80$, and upper time limit $T = 25$. Price Path 1 crosses the optimal harvest boundary B_{τ^*} at $\tau^* = 10$ and contributes to the first sum of Simulation 3. Price Paths 2 and 3 contribute to the second sum, because $\tau^* = 25$ in both cases. The terminal value of Price Path 3, S^3_{25}, is below the harvest cost, and a rational forest owner would leave the stand

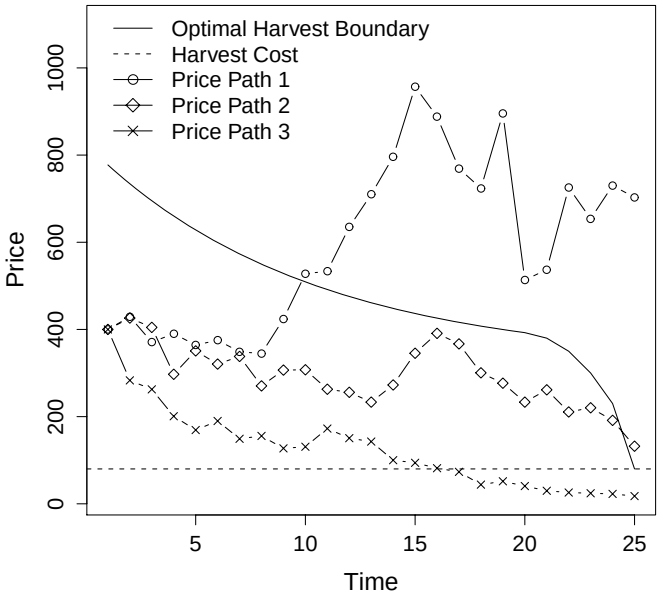

Figure 1: Monte Carlo procedure for calculating the average discounted value of a single rotation harvest contract.

unharvested under that price scenario. Hence, the contribution of Price Path 3 to the value of $\pi(S_0, C)$ is equal to zero.

The implementation of Simulation 3 proceeds as follows. First, the price model of Equation 2 is used to simulate M price paths. For the L price paths that cross the boundary B_t at a $\tau^* < T$, the profit from immediate harvest at τ^* is recorded. For the K price paths that reach T without crossing B_t, the time T harvest profit is recorded, if positive. If it is negative, its value is recorded as zero. All profit values are then appropriately discounted to time zero, and the estimate of the option value $\pi(S_0, C)$ is calculated as their average.

The optimal harvest boundary B_t can be recovered by using Simulation 3 recursively. Because the stand value at the terminal time T can be calculated as $Q_T(S_T - C)^+$, the first point where B_t has to be calculated is $t = T - 1$. This boundary point is calculated by finding the price of timber, S^*_{T-1}, at which

$$\begin{aligned}Q_{T-1}(S^*_{T-1} - C)^+ = \\ \mathbb{E}[d^T_{T-1} Q_T (S_T - C)^+ | S^*_{T-1}, C]\,,\end{aligned} \tag{4}$$

that is, the price where the value of immediate harvest is exactly equal to the expected discounted value of harvesting at time T. Thus, from a computational perspective, finding the value of the optimal harvest boundary at time $T - 1$ is a root-finding problem in S^*_{T-1}, and the calculation yields $B_{T-1} = S^*_{T-1}$. For a given value of S_{T-1}, the value of immediate harvest at time $T - 1$,

on the left side of Equation 4, is easily calculated, because all necessary quantities are known at $T-1$. The expected value of delayed harvest on the right side of Equation 4 can be approximated by the simulation

$$\mathbb{E}[d_{T-1}^{T} Q_T (S_T - C)^+ | S_{T-1}] \approx \frac{1}{M} \sum_{i=1}^{M} d_{T-1}^{T} Q_T (S_T^i - C)^+ , \quad (5)$$

the average of discounted profit values from harvesting at time T. This simple approximation of the expectation term is possible because during the short time interval $(T-1, T)$, it is assumed that the stand cannot be harvested and, hence, the optimal harvest boundary need not be used.

With B_{T-1} known, a step is taken back in time to $t = T-2$, and the process is repeated for B_{T-2}. The value of immediate harvest at time $T-2$, on the left of Equation 4, is compared to the expected value of delayed harvest. Because harvest is now possible not only at $t = T$ but also at $t = T-1$, the simple Simulation 5 cannot be used this time around, and the time $T-2$ expectation must approximated with

$$\pi(S_{T-2}, C) \approx \frac{1}{M} \sum_{i=1}^{L} d_{T-2}^{\tau^*} Q_T (S_{\tau^*}^i - C) + \frac{1}{M} \sum_{j=1}^{K} d_{T-2}^{T} Q_T (S_T^j - C)^+ , \quad (6)$$

with $\tau^* = T-1$ and the optimal harvest boundary specified by $B_{T-1} = S_{\tau^*}^*$. Note that Simulation 6 is a special case of Simulation 3, implemented for $\tau^* \in \{T-2, T-1, T\}$ and the starting value of timber price set equal to S_{T-2}.

The value of the optimal harvest boundary at times $T-3, T-4, \ldots 1, 0$ is calculated through similar steps, each time utilizing the knowledge of B_t acquired at previous time points. Once the entire boundary B_t is known, it can be used to approximate the option value as described in Simulation 3.

3 Multiple Rotations

The Ibáñez and Zapatero algorithm described in the preceding section provides an effective tool for solving the single rotation stochastic optimal harvest problem with the substitution of harvest cost for the strike price and the introduction of Q_t. However, it cannot be applied to the more relevant multi-rotation optimal harvest problem without further modifications. This section presents the changes that must be made to the algorithm in order to apply it to the multi-rotation optimal harvest problem with stochastic timber prices.

The extended algorithm consists of several steps. First, it is necessary to determine N, the number of rotations that will be considered in the calculations. Although there is no theoretical limit on the value of N, computational considerations dictate that N be finite. Hence, N must be determined empirically, as a tradeoff between accuracy and computational cost.

For a given value of N, the multi-rotation method starts at the N^{th} rotation and proceeds backward through the rotations until the first rotation is reached. First, estimates of $\pi^N(S_0, C)$, the value of the N^{th} rotation, as well as the corresponding optimal harvest boundary B_t^N are calculated for a set of initial timber prices S_0 with the method presented in the preceding section. The calculated values of $\pi^N(S_0, C)$ are then interpolated to provide an estimate of

$$f^N(S_0 | C, r, b(t, S_t), \sigma(t, S_t), \ldots) \approx \pi^N(S_0, C) , \quad (7)$$

the N^{th} harvest value as a function of the starting price of timber S_0 for given values of harvest cost C, discount rate r, drift coefficient $b(t, S_t)$, volatility $\sigma(t, S_t)$, and all other relevant quantities.

In the next step, the value of $\pi^{N-1}(S_0, C)$, the second-to-last harvest, is calculated together with its associated optimal harvest boundary function B_t^{N-1}. In the boundary calculations, the root-finding procedure of Equation 4 is modified by incorporating the discounted value of the N^{th} harvest as estimated by Approximation 7. For a given stand age t, the value of the optimal harvest boundary B_t^{N-1} is given by the root of the equation

$$Q_{t-1}(S_{t-1}^* - C)^+ + f^N(S_{t-1}^* | \cdot) = \mathbb{E}[d_{t-1}^{t} \{Q_t (S_t - C)^+ + f^N(S_t | \cdot)\} | S_{t-1}^*, C] . \quad (8)$$

Equation 8 states that at any point t on the optimal harvest boundary for the $N-1^{th}$ rotation, B_t^{N-1}, the sum of profit from harvesting at time $t-1$ and the expected discounted value of the N^{th} harvest, $f^N(S_t | \cdot)$, must equal the expected discounted value of the equivalent sum for time t.

Analogous changes are made to the contract valuation procedure of Simulation 3 in order to introduce the impact of the N^{th} rotation. At harvest time, the forest owner now receives not only the value of $N-1^{th}$ harvest but also the expected discounted value of the final, N^{th}, harvest approximated by

$$\pi^{N-1}(S_0, C) \approx \frac{1}{M} \sum_{i=1}^{L} d_0^{\tau^*} \{Q_{\tau^*}(S_{\tau^*}^i - C) + f^N(S_{\tau^*}^i | \cdot)\} + \frac{1}{M} \sum_{j=1}^{K} d_0^{T} \{Q_T (S_T^j - C)^+ + f^N(S_T^j | \cdot)\} . \quad (9)$$

Equation 8 and Simulation 9 are used recursively to recover the entire length of the optimal harvest boundary B_t^{N-1} for the $N-1^{th}$ rotation, which is then used to calculate the combined value of the last two harvests for a set of starting values of timber price S_0. The results are interpolated to provide

$$f^{N-1}(S_0|C, r, b(t, S_t), \sigma(t, S_t), \ldots) \approx \pi^{N-1}(S_0, C)\,, \tag{10}$$

an estimate of the combined value of the $N-1^{th}$ and N^{th} harvests as a function of initial timber price.

In the next step, the expression on the left of Approximation 10 is substituted in place of $f^N(\cdot)$ in Equation 8 and Simulation 9. The revised relations are then used to obtain the optimal harvest boundary B_t^{N-2} for the $N-2^{nd}$ rotation and the corresponding estimate of the combined value of the last three harvests, $f^{N-2}(S_0|\cdot)$ as a function of starting timber price.

The procedure described above is repeated until the first rotation is reached. The optimal harvest boundary for the first rotation B_t^1 is recovered with the use $f^2(S_0|\cdot)$, the estimate of the combined expected discounted value of $N-1$ future rotations, and can be used to calculate

$$f^1(S_0|C, r, b(t, S_t), \sigma(t, S_t), \ldots) \approx \pi^1(S_0, C)\,, \tag{11}$$

the expected bare land value as a function of the current timber price.

As the value of the number of rotations N increases, the expression on the left of Approximation 11 provides an ever more accurate estimate of the solution to the infinite-rotation optimal harvest problem with stochastic timber prices. Thus, the methodology described in this section provides a Monte-Carlo counterpart to the finite-difference methodology typically used to solve this problem, for example as demonstrated by Insley and Rollins 2005.

4 Second Risk Source

One of the strengths of the original Ibáñez and Zapatero algorithm is its ability to solve problems characterized by the presence of multiple risk sources. This property is retained by the multi-rotation version introduced in Section 3.

In addition to stochastic timber prices, there are many other sources of risk that could be included in the formulation of the optimal timber harvest problem. These include, for example, stochastic discount rate r, yield function Q_t, and harvest cost C. Another potentially significant source of risk can be introduced via the price of carbon emission permits. Forests act as carbon sinks, and the ability to sequester carbon could put forest owners in a position to act as suppliers of permits in the carbon emission markets. This section details the steps necessary to apply the multi-rotation algorithm to a two-dimensional stochastic optimal harvest problem with stochastic timber and carbon prices.

Under the carbon accounting system assumed in this article, each year a forest stand goes unharvested, its owner receives sequestration credit for the additional volume of carbon the stand has absorbed. This credit can then be sold in the carbon emissions market. The resulting cashflow

$$CF_U^t = \gamma\,\Delta\,Q_t\,U_t \tag{12}$$

is received by a forest owner who decides not to harvest at time t. In Equation 12, γ represents a factor for converting atmospheric CO_2, measured in metric tons, to carbon sequestered in the forest stand and measured in thousand board feet, MBF; $\Delta\,Q_t$ represents the additional volume of timber accumulated in the forest stand over the period from time $t-1$ to time t; and U_t stands for the price of CO_2 emissions per metric ton at time t.

If the owner decides to harvest the stand at t, the cashflow from immediate harvest, CF_S^t, is calculated as

$$CF_S^t = Q_t(S_t - \alpha\,\gamma\,U_t - C)^+, \tag{13}$$

where α represents the percentage of carbon sequestered in the stand that is released at harvest time and all other parameters are as defined above. Equation 13 implies that a stand harvest is to be treated as a carbon source, and the term $\alpha\,\gamma\,U_t$ represents the cost of the carbon emission permits the forest owner must purchase at harvest time.

In the univariate stochastic harvest problem of Section 3, the optimal harvest boundary B_t^1 is formed by a single curve. For a given stand age t where harvesting is possible, there exists a unique threshold timber price S_t^* above which the stand should be harvested immediately. In the problem with two sources of risk, the optimal harvest boundary consists of two sets of functions. For each stand age t, the optimal harvest boundary must be specified by a pair of functions

$$U^* = g^t(S_t) \tag{14}$$

and

$$S^* = h^t(U_t)\,. \tag{15}$$

If, at a given stand age t and timber price S_t, the price of CO_2, U_t, falls below the threshold price U^*, the stand is harvested immediately. Similarly, the stand is harvested immediately if, for a given stand age t and CO_2 price U_t, the price of timber S_t exceeds the threshold price S^*.

Assuming, as in the one-dimensional case, that initial prices of timber, S_0, and carbon, U_0, are the only simulation inputs that vary from one rotation to the

next, introducing carbon permits as a second source of stochastic revenue turns the expected bare land value, f^1, into a function of two variables

$$f^1(S_0, U_0|C, r, b_S, \sigma_S, \ldots) \approx \pi^1(S_0, U_0, C)\,. \qquad (16)$$

That is, $f^1(S_0, U_0|\cdot)$ now defines a surface over the S_0, U_0-plane for given values of the harvest cost C, discount rate r, price trends b_S, b_U, volatilities σ_S, σ_U, and other parameters.

The expected bare land value of Approximation 16 represents a two-dimensional analog of Approximation 11 and can be calculated with a procedure similar to the one used in the univariate case. For a given number of rotations, N, the procedure starts with the N^{th} rotation and recursively calculates expected bare land values and associated boundary functions until the first rotation is reached. For each rotation $i \in 1, \ldots, N$, an estimate of the optimal harvest boundary at a given age t, consisting of two sets of age-specific optimal harvest curves of Equations 14 and 15, is calculated, together with an estimate of the value function $f^i(S_0, U_0|\cdot)$.

Given a rotation i, a boundary curve $g^t(S_t)$ specified in Equation 14 can be calculated at each stand age t, by holding the timber price fixed at a particular value, $\bar{S}_t \in \bar{\mathbb{S}}_t$, while searching for the root U^* by varying the value of U_t. The set $\bar{\mathbb{S}}_t$ consists of all points on the S_t axis where the boundary is to be calculated for a given stand age t. Thus, the boundary search in the carbon direction consists of finding the root U^* of equation

$$\begin{aligned} CF_S^t + f^{i+1}(\bar{S}_t, U^*|\cdot) = CF_U^t + \\ \mathbb{E}[d_t^{t+1}\{CF_S^{t+1} + f^{i+1}(S_{t+1}, U_{t+1}|\cdot)\}|\bar{S}_t, U^*]\,, \end{aligned} \qquad (17)$$

where the timber and carbon cashflows CF_S^t and CF_U^t are specified by Equations 12 and 13, and the value of $f^{i+1}(S_t, U_t|\cdot)$ is known from previous calculations. Equation 17 states that, for each point on the optimal boundary, the sum of the harvest profit at time t, CF_S^t, and the expected discounted value of future rotations, $f^{i+1}(\cdot|\cdot)$ must equal the value of carbon payment, CF_U^t and the expected discounted value of delayed harvest. This root-finding procedure is performed for all values of $\bar{S}_t \in \bar{\mathbb{S}}_t$. The calculated values of U^* can then be interpolated to produce an approximation of $g^t(S_t)$, the age-specific optimal harvest boundary in the carbon direction of Equation 14.

Once the boundary curve in the carbon direction is known, the roles of S_t and U_t are reversed. A boundary curve $h^t(U_t)$ of Equation 15 is found by holding carbon price fixed at a particular value $\bar{U}_t \in \bar{\mathbb{U}}_t$ and finding the root S^* of equation

$$\begin{aligned} CF_S^t + f^{i+1}(S^*, \bar{U}_t|\cdot) = CF_U^t + \\ \mathbb{E}[d_t^{t+1}\{CF_S^{t+1} + f^{i+1}(S_{t+1}, U_{t+1}|\cdot)\}|S^*, \bar{U}_t]\,, \end{aligned} \qquad (18)$$

by varying the price of timber. This root-finding procedure is also performed for all values $\bar{U}_t \in \bar{\mathbb{U}}_t$, with $\bar{\mathbb{U}}_t$ being the set of points on the U_t axis where the boundary is to be calculated for a given stand age t. The resulting values of S^* can be interpolated to yield an estimate of the age-specific boundary curve in the timber direction of Equation 15.

An estimate of the expectation term on the right of Equations 17 and 18 is calculated as

$$\pi^i(S_t, U_t, C) \approx \frac{1}{M}\sum_{v=1}^{L} T_v + \frac{1}{M}\sum_{r=1}^{K} E_r \qquad (19)$$

which is a two-dimensional analog of Simulation 9 with $T_v = \sum_{w=1}^{\tau^*-1} d_t^w CF_{U,v}^w + d_t^{\tau^*}\{CF_{S,v}^{\tau^*} + f^{i+1}(S_{\tau^*}^v, U_{\tau^*}^v|\cdot)\}$ and $E_r = \sum_{z=1}^{T-1} d_t^z CF_{U,r}^z + d_t^T\{CF_{S,r}^T + f^{i+1}(S_T^r, U_T^r|\cdot)\}$. In Simulation 19, $M = K + L$ is the number of simulated bivariate price paths. K stands for the number of price paths that did not lead to early harvests at times $t \le \tau^* < T$, while L represents the number of price paths where such early harvests occurred. Each of the terms $\sum_{i=1}^{U-1} d_t^i CF_{U,j}^i$ represents the discounted value of all annual carbon cashflows of Equation 12 that were accrued before a harvest took place for a given price path j either because carbon price falls below the optimal harvest boundary, *i.e.* $U_{\tau^*} \le U^*$, or timber price exceeds the optimal harvest boundary, *i.e.* $S_{\tau^*} \ge S^*$. All other terms are defined as above.

Once a pair of boundary curves is calculated for every stand age $t \in \{0, \ldots, T\}$ for a given rotation i, the boundary curves can be used to find the bare land value $\pi^i(S_0, U_0, C)$ with Simulation 16, which represents the second part of the solution for rotation i. The procedure of calculating the optimal harvest boundary and associated expected bare land value is repeated recursively for all rotations $i \in \{1, \ldots, N\}$ starting at $i = N$ and terminating at $i = 1$. The expected bare land value of the first rotation, $\pi^1(S_0, U_0, C)$, together with the associated set of boundary curves represent the solution of the infinite horizon optimal harvest problem with stochastic timber and carbon prices.

5 Illustrative Example

In order to illustrate the application of the bivariate algorithm presented above to a forest management problem, it was necessary to identify several key inputs. The first of these concerned the site location and silviculture.

The forest stand used in this study was assumed to be located on a high yield site in western Washington State. A yield curve appropriate for such a location was approximated by spline fitting from a dataset spanning a 100 year period. The available yield data determined the length of simulation horizon, T, which was set to 100

Table 1: Silvicultural and other site specific information.

Silviculture	
Property	*Value*
Location	Western Washington
Site Yield	High
Composition	100% Douglas fir
Management Regime	Clearcut

Table 2: Forest owner specific parameters.

Forest Owner Characteristics	
Parameter	*Value*
Replanting and Harvest Cost ($/MBF)	100
Annual Discount Rate (%/year)	5
Time Step Length (year)	1

years, with five years being the earliest possible harvest age producing commercially valuable timber. The stand was assumed to be 100% composed of Douglas fir, and the management regime to consist of clearcut harvests followed by immediate replanting. In all calculations, there was assumed to be one harvest opportunity every year between the stand ages of five and 100 years. Table 1 provides a summary of site specific properties.

Other parameters whose values had to be specified include the appropriate annual rate of discount and the magnitude of the harvest and replanting cost per MBF. Both of these parameters were assumed to vary across forest owners. In particular, the rate of discount was assumed to reflect the cost of capital to a given forest land owner rather than the risk-free rate. The values used in this article are given in Table 2.

In order to calculate the cashflows from Equations 12 and 13, it was necessary to specify the values of α and γ. α represents the percentage of sequestered carbon removed from the stand at harvest time, and its value was set to 60% by assumption. γ is a factor for converting atmospheric CO_2 in metric tons to sequestered carbon in MBF of Douglas fir. Its value was determined from available data.

The prices of carbon and timber were modeled by the logarithmic mean-reverting stochastic process. The logarithmic mean-reverting process is conveniently described by the stochastic differential equation

$$dS_t = \kappa\left(\mu - \ln S_t\right) S_t\, dt + \sigma\, S_t\, d\mathbb{W}_t\,, \qquad (20)$$

where S_t represents the price at time t, κ stands for the rate of reversion to the long term trend μ, σ stands for price volatility, and $d\mathbb{W}_t$ is an increment of the Wiener process.[2]

[2]From the perspective of microeconomic theory, the logarithmic mean-reverting process is an attractive choice for the price of timber – a renewable resource. However, the model was chosen for carbon prices only as a proxy, to be replaced by a more appropriate process when more data becomes available.

Table 3: Forest-owner-specific parameters.

Carbon Parameters	
Parameter	*Value*
α (%)	60
γ (CO_2 ton/MBF)	3.6

Using Ito's lemma, Equation 20 can be solved analytically. The exact transitional density of $\ln S_t$ is normal and takes on the form

$$\ln S_t \sim \mathbb{N}(\Theta;\, \Sigma)\,, \qquad (21)$$

where $\Theta = \ln S_0 + (1 - e^{-\kappa t})(\mu - \sigma^2/2\kappa)$ and $\Sigma = \sigma\sqrt{(1 - e^{-2\kappa t})/2\kappa}$. Because the distribution defined in Model 21 is the exact solution of Equation 20, it can be used to simulate price paths of S_t with an arbitrary step length, such as the one year length used in our simulations.

Table 4 contains the price model parameter values that were used during the simulations. These values were estimated from stumpage price data by linear regression. The only exception was ρ, which denotes the strength of the correlation between the elements of the bivariate Wiener process used in simulating the price paths of timber and carbon. The value of ρ was set to 10% by assumption, because the available time series did not overlap.

After the price model was chosen and calibrated, it was used to determine $\bar{\mathbb{S}}_t$ and $\bar{\mathbb{U}}_t$, the sets of points on the S_t and U_t axis where the boundary curves of Equations 14 and 15 would have to be calculated. The simplest way to determine $\bar{\mathbb{S}}_t$ and $\bar{\mathbb{U}}_t$ is to use Model 21 to simulate a large number of price paths over the entire length of the simulation horizon, in this case 100 years. Figure 2 contains a plot of the terminal values of 10,000 price paths from a typical simulation performed with the parameters set to values specified in Table 4.

The plot in Figure 2 shows that very few price paths terminated outside the rectangle whose upper right corner was located at the $2000 dollar mark in the timber direction and the $100 mark in the CO_2 direction. These values were used to establish empirical upper limits of the domains of the optimal harvest boundaries of Equations 14 and 15. The set $\bar{\mathbb{S}}_t$ was then formed from 40 values of S_t evenly spaced in the interval $S_t \in [0, 2000]$. Similarly, the set $\bar{\mathbb{U}}_t$ was formed from 20 values of U_t evenly spaced in the interval $U_t \in [0, 100]$.

The product $\bar{\mathbb{S}}_t \times \bar{\mathbb{U}}_t$ defines a grid of points in the S_t, U_t-plane where the estimates of the expected bare

Table 4: Parameter values for stochastic differential equations governing the behavior of timber and carbon prices.

Price Model Parameters		
Parameter	Timber	Carbon
S_0	400 (\$/MBF)	25 (\$/CO_2 ton)
μ	6.0 (ln \$/MBF)	3.5 (ln \$/CO_2 ton)
κ (%/year)	0.35	4.0
σ (%/year)	0.4	0.5
ρ (%/year)	0.1	

land value functions $f^i(S_0, U_0|\cdot)$ would have to be calculated in order to evaluate Simulation 19.[3]

6 Simulation Results

The mean reversion property of the price model specified by Equation 20, combined with the long time horizons characteristic of the optimal timber harvest problem, suggests that current prices of timber and carbon should have only a small impact on expected bare land values, $f^i(S_0, U_0|\cdot)$, for all but very low values of mean reversion rate κ. Instead, the long term price level μ should be the price model parameter most influential in determining bare land values.

In order to test this intuition, the expected bare land value of a single rotation ($N = 1$) was calculated for different pairs of starting timber and carbon prices on a 50×50 grid spanning the $(0, 2000) \times (0, 100)$ region of the S_t, U_t-plane. Four such simulations, each with re-initialized starting value of the random number generator, were performed in *R* **?**. In each of the four simulations, a visual inspection of the results revealed no pattern, and the differences in the values of $f^i(S_0, U_0|\cdot)$ surface appeared to be caused by the random variation characteristic of Monte-Carlo results. A regression plane was fitted to each of the four datasets. All four planes were nearly flat over the region of interest, and there was no discernible pattern in the direction of the normal vector: each of the planes was slightly tilted in a different direction.

These results indicate that, for mean reverting processes, the initial prices of timber and CO_2 have only a minimal impact on expected bare land values with the simulation parameters as given above. This leaves the constant long-term price trend μ, price volatility σ, rate of discount, and site productivity as the factors that determine bare land values. Because the expected bare land value surface is nearly flat over the relevant region of the S_t, U_t-plane, its estimate $f^1(S_0, U_0|\cdot)$ need not be calculated in its entirety over a large grid of starting timber and carbon prices. It is sufficient to calculate $f^1(S_0, U_0|\cdot)$ at a single point (S_0, U_0) located, for example, near the center of the region of interest. This approach greatly reduces the amount of calculations required to estimate $f^1(S_0, U_0|\cdot)$ as well as the estimates of future rotation values $f^i(S_0, U_0|\cdot)$ for $i \in 2, \ldots, N$.

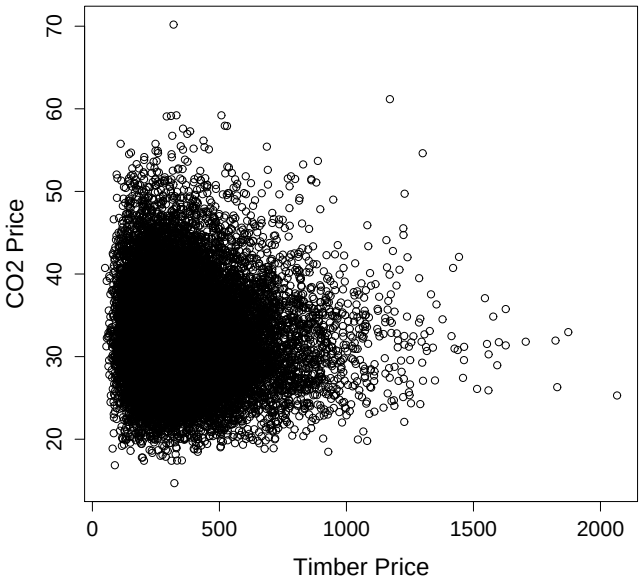

Figure 2: Estimate of the region containing the majority of end values of 50,000 timber and carbon price paths simulated over a period of 100 years.

Another potentially significant reduction of computational effort may be realized by judiciously choosing N, the number of rotations. Performing several simulations for increasing values of N can help assess the rate of convergence in the number of rotations. The results of these simulations for parameter values of Tables 1 through 4 are illustrated in Figure 3.

Each of the box-plots in Figure 3 was constructed from the results of nine sample runs. The first box-plot represents the value of a single rotation. The second box-plot represents the combined value of two rotations, the third box-plot represents the combined value of three rotations, and so on. The figure reveals that for the parameter values specified above, convergence is achieved by simulating four harvests, and tolerable accuracy is achieved by simulating three harvests.

[3]For price models such as in Equation 20 that permit an analytical solution, these ranges can be determined exactly from the transitional density for a desired confidence level. However, this empirical procedure works well for more complex price models where the exact form of the transitional density is unavailable.

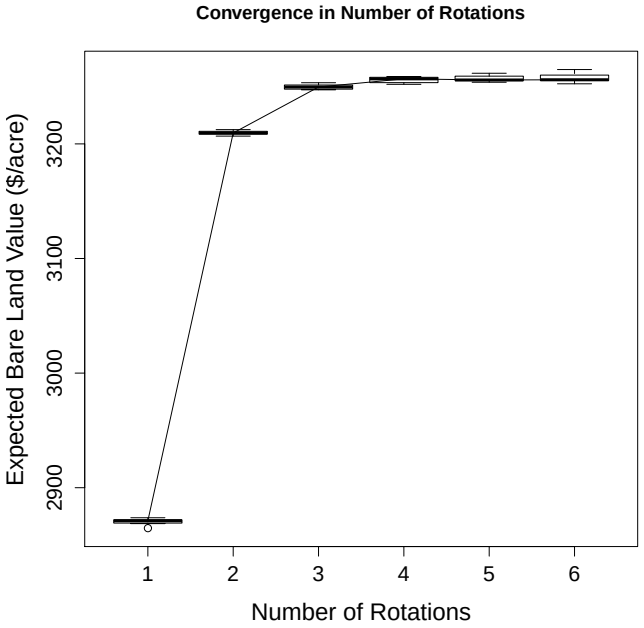

Figure 3: Convergence is achieved after four rotations (*i.e.* $N = 4$). Each of the six box-plots indicating the combined value of future harvests was generated from nine sample runs.

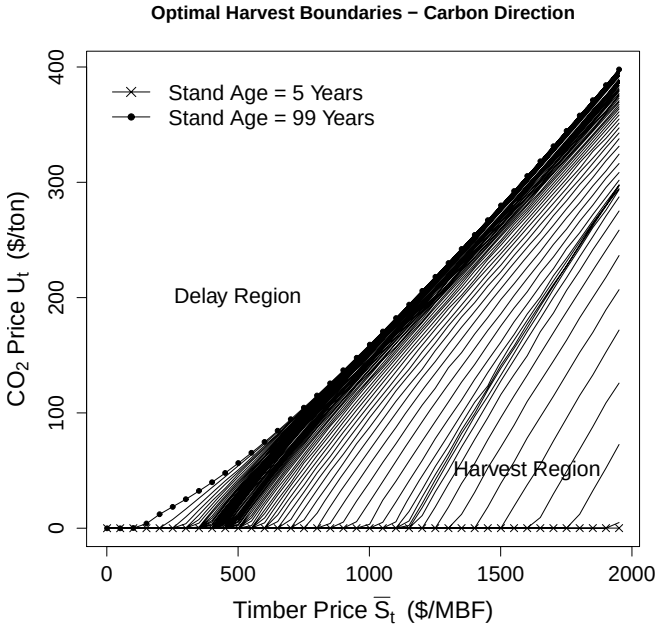

Figure 4: Each $g^t(S_t)$ curve initially runs along the horizontal axis and then deviates upward. Note that the size of the delay region decreases with increasing stand age.

As discussed previously, the solution to the stochastic optimal harvest problem consists not only of the expected bare land value but also of the optimal harvest boundary, which serves as a decision-making rule for the forest owner with regard to optimal harvest timing. The shape of the optimal harvest boundary curves for the stand used in this analysis is revealed by Figures 4 and 5. The boundary curves in Figure 4, specified by Equation 14, were calculated for 40 evenly spaced values of the timber price $\bar{S}_t \in [0, 2000]$. The boundary curves in Figure 5, specified by Equation 15, were calculated for 20 evenly spaced values of the CO_2 price $\bar{U}_t \in [0, 100]$. All intermediate values were approximated by linear interpolation.

For a given stand age t, each of the optimal harvest boundaries depicted in Figure 4 separates the S_t, U_t-plane into harvest and delay regions. As described in the previous section, a point on a boundary curve is calculated by holding the selected timber price fixed at $\bar{S}_t$ while searching for the corresponding carbon price U^* that equalizes value of harvesting today with the expected discounted value of harvesting harvesting later. The region below a given curve is the harvest region, because in this area timber prices are high relative to carbon prices. In the region above the curve is the delay region, because the revenue from carbon sequestration is relatively high there. Note that as the stand age increases, the size of the harvest region increases at the expense of the delay region, *i.e.* a mature stand is more likely to get harvested.

The optimal harvest boundary curves depicted in Figure 5 are obtained, for a given stand age t, by fixing the price of carbon at $\bar{U}_t$ while searching for the price of timber S^* that equalizes the value of harvesting immediately and the expected discounted value of harvesting later. As in the previous case, each of the boundary curves separates the price plane into harvest and delay regions. However, in Figure 5, the harvest region is above each curve, because carbon prices are relatively low there and do not justify further harvest delay. Hence, the stand should be harvested immediately if timber prices are above the boundary. The delay region is located below the boundary curve where carbon prices are relatively high and timber prices relatively low, thus harvest should be delayed to maximize revenue from carbon payments. As before, the area of the harvest region increases as the stand matures.

The last result presented in this section concerns the distribution of optimal harvest ages. In the traditional Faustmann framework, timber prices are known and

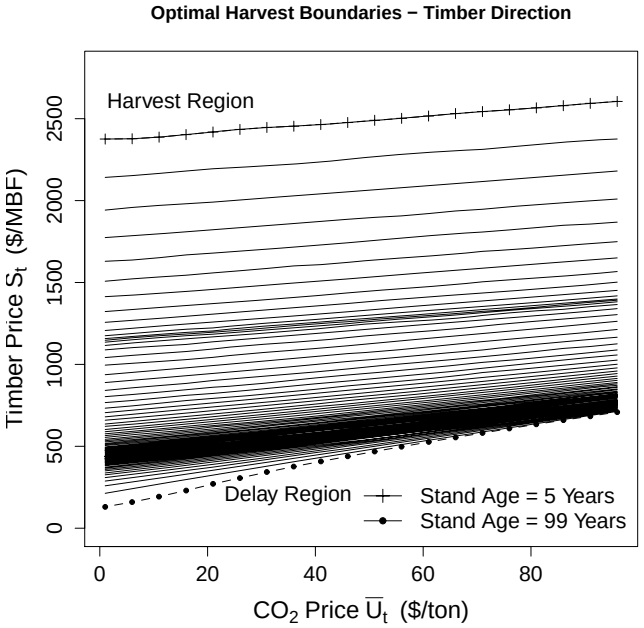

Figure 5: Each $h^t(U_t)$ curve separates the price plane into delay and harvest regions for a given age of the stand t. Note the decrease in the size of the delay region with increasing stand age.

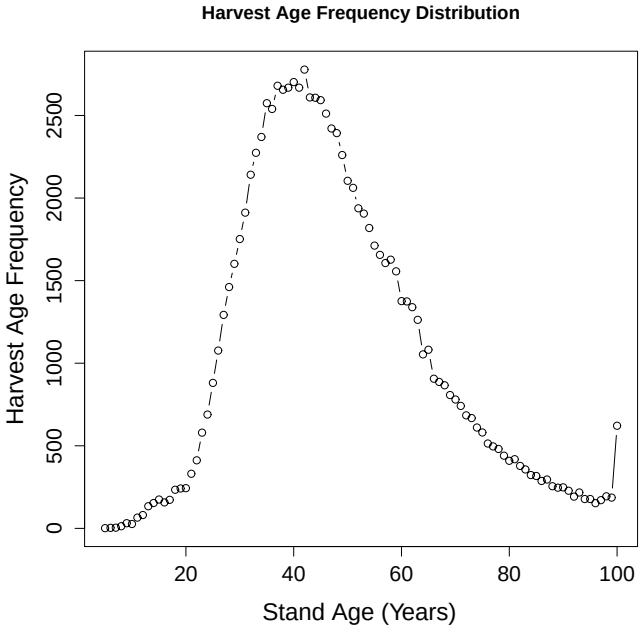

Figure 6: Frequency distribution of harvest timings for 50,000 simulated price paths with corresponding 50,000 antithetic paths. The typical harvest age for the stand used in the analysis is about 45 years.

constant and, hence, a fixed optimal rotation length can be determined. Such a strong result cannot be obtained when prices are stochastic. In order to maximize profit, forest owners must adjust harvest timings in response to price fluctuations. Figure 6 depicts the frequency distribution of recorded harvest ages for a sample simulation run and indicates that, given the above values of simulation parameters, the mode harvest age is about 40 years. In order to reveal the full shape of the harvest time distribution, the minimal harvest age was set equal to two years, even though the commercial value of the stand at that age is minimal. The sudden increase in the number of harvests at the end of the simulation horizon is an artifice of the finite simulation horizon that would not be observed in reality.

7 Summary

This article presented a Monte-Carlo-based methodology for the solution of the multi-period optimal harvest problem with stochastic prices of timber and CO_2. The solution algorithm extends the work of Ibáñez and Zapatero 2004 and provides a flexible alternative to the numerical methods based on finite difference schemes that have been previously employed in the literature.

For illustrative purposes, the methodology was employed to calculate the expected bare land value for a Douglas fir stand that was assumed to be located on a high yield site in western Washington State. In addition to calculating expected bare land values, the optimal harvest boundaries used for decision making with regard to harvest timing were also calculated for each age where harvesting the stand is possible. The results of expected bare land value calculations and the optimal harvest boundaries were then discussed. Additionally, a frequency distribution of optimal harvest ages was presented and discussed.

In the analysis, the prices of timber and CO_2 were each assumed to follow a logarithmic mean-reverting process. While the logarithmic mean-reverting process is a realistic choice for the model of timber price behavior, it was used only as a proxy in the case of carbon prices. Further analysis is necessary in order to identify a more appropriate model of carbon prices. At present time, however, this task is made difficult by lack of requisite data. When a new model of carbon prices has been identified, it should be easily incorporated into the described methodology to yield more accurate results.

8 Acknowledgements

The authors would like thank two anonymous reviewers for helpful comments on the manuscript. The authors are solely responsible for any remaining errors.

References

Brazee, R. J., and D. H. Newman, 1999. Observation on recent forest economics research on risk and uncertainty. Journal of Forest Economics 5(2):193–200.

Chladna, Z., 2007. Determination of optimal rotation period under stochastic wood and carbon prices. Forest Policy and Economics 9(8):1031–1045.

Dixit, A., and R. Pindyck, 1994. Investment under Uncertainty. Princeton University Press, Princeton, NJ.

Glasserman, P., 2004. Monte Carlo Methods in Financial Engineering. Springer-Verlag, New York.

Haight, R. G., 1993. The economics of Douglas-fir and red alder management with stochastic price trends. Canadian Journal of Forest Research 23:1695–1703.

Hull, C., John, 2003. Options, Futures, and Other Derivatives. Prentice Hall, Upper Saddle River, NJ.

Ibáñez, A., and F. Zapatero, 2004. Monte Carlo valuation of American options through computation of the optimal exercise frontier. Journal of Financial and Quantitative Analysis 39(2):253–275.

Insley, M., 2002. A real options approach to the valuation of a forestry investment. Journal of Environmental Economics and Management 44:471–492.

Insley, M. C., and K. Rollins, 2005. On solving the multirotational timber harvesting problem with stochastic prices: A linear complementarity formulation. American Journal of Agricultural Economics 87(3):735–755.

Kaya, J., and J. Buongiorno, 1987. Economic harvesting of uneven-aged northern hardwood stands under risk: A Markovian decision model. Forest Science 33:889–907.

Lohmander, P., 1987. The economics of forest management under risk. Report 79, Swedish University of Agricultural Sciences, Department of Forest Economics, Umea.

Morck, R., E. Schwartz, and D. Stangeland, 1989. The valuation of forestry resources under stochastic prices and inventories. The Journal of Financial and Quantitative Analysis 24(4):473–487.

Newman, D. H., 1988. A discussion of the concept of the optimal forest rotation and a review of the recent literature. General Technical Report SE-48, USDA Forest Service, Southeastern Forest Experiment Station.

Norstrom, C. J., 1975. A stochastic model for the growth period decision in forestry. The Swedish Journal of Economics 77(3):329–337.

Plantinga, A. J., 1998. The optimal timber rotation: An option value approach. Forest Science 44(2):192–202.

Trigeorgis, L., 1996. Real options: Managerial flexibility and strategy in resource allocation. The MIT Press, Cambridge, MA.